Excitation of surface plasmon polaritons along the sinusoidal boundary of a metamaterial

Mauro Cuevas* and Ricardo A. Depine†
Grupo de Electromagnetismo Aplicado, Departamento de Física, Facultad de Ciencias Exactas y Naturales, Universidad de Buenos Aires, Ciudad Universitaria Pabellón I, 1428 Buenos Aires, Argentina
(Received 8 March 2008; revised manuscript received 4 June 2008; published 17 September 2008)

We present a detailed analysis about the excitation of surface polaritons (SPs) at the sinusoidally corrugated interface between a conventional dielectric medium and a metamaterial (MM) with arbitrary values of dielectric permittivity and magnetic permeability. The strong impact of SPs on the optical response of the interface is demonstrated by numerical examples obtained with a rigorous electromagnetic code. Conditions leading to total absorption of the incident power and to near-field enhancements are explored in new SP regimes provided by the emergence of MMs. In those regimes where waves incident on the surface without corrugation suffer reactive attenuation, we find SP effects very similar to those occurring for metallic gratings, where the introduction of a weak corrugation in an otherwise highly reflecting surface can turn its reflectivity to zero. New SP effects are identified in regimes corresponding to ideally transparent MMs with a negative index of refraction. In these regimes, contrary to the case of metallic gratings, the introduction of a weak corrugation in an otherwise poorly reflecting surface produces high reflectivities in angular regions corresponding to SP excitation. Moreover, maximal absorption of incident waves and maximal intensity of the excited SP do not occur under the same conditions in these regimes. The complex propagation constants of the SPs supported by the corrugated interface are approximately obtained by fitting a phenomenological expression to our numerical results.

DOI: 10.1103/PhysRevB.78.125412 PACS number(s): 78.68.+m, 73.20.Mf, 42.79.Dj, 42.25.Ja

I. INTRODUCTION

It is known that, under certain particular conditions, the interface between two different isotropic dielectric materials can support the propagation of surface polaritons (SPs), which is electromagnetic waves that propagate along the interface with their electric and magnetic fields strongly localized near the interface. Most of the literature in this field (see Refs. 1–5, and references therein) has been devoted to *p*- (or TM-) polarized SPs, which occur at interfaces between isotropic materials with opposite signs of the real part of their dielectric permittivities, i.e., between insulators (positive permittivity) and metals or plasmas below a critical frequency (generally complex permittivity with a negative real part). These SPs propagate with a wave vector greater than that corresponding to a free space photon of the same frequency, and therefore, they are nonradiative modes that cannot be excited by light on a flat surface.

Apart from the well-known *p*-polarized SP supported by insulator-metal interfaces, *s*- (or TE-) polarized SPs can be excited if the materials separated by the interface have a real part of their magnetic permeabilities with opposite signs.[6] This condition cannot be easily attained with conventional—generally nonmagnetic—materials, which is why the vast majority of research in the last century was focused on *p*-polarized SPs involving nonmagnetic media.

Possibilities have been widened with the recent advent of metamaterials (MMs), artificially constructed composites exhibiting electromagnetic properties that are difficult or impossible to achieve with conventional naturally occurring materials.[7–10] Key representatives of this class of materials are MMs with negative index of refraction, a property that arises in nonabsorbing media with a negative electric permittivity together with a negative magnetic permeability in the same frequency range. For actual absorbing MMs, the relation that must be satisfied to obtain a negative index of refraction is a more relaxed one.[11] MMs capable of producing negative refraction in different bands of the terahertz range are currently being fabricated, and their properties tested in different laboratories around the world. A list of selected developments—starting from Ref. 12 at 4.85 GHz and covering up to Ref. 13 at 380 THz, i.e., the red end of the visible spectrum—was published in a recent paper by Tsukerman.[14] MMs exhibiting negative index of refraction and low losses even in the visible range of the spectrum have been recently proposed.[15]

Ruppin[6] noted that the interface between a conventional material and a MM with negative index of refraction could support the propagation of SPs not only for *p* but also for *s* polarization. General conditions for the existence of SPs at the flat interface of lossless, isotropic MMs with negative index of refraction together with the identification of new SP regimes have been presented in Refs. 16 and 17. In this paper we distinguish six SP regimes for flat interfaces between a lossless conventional material, with electric permittivity ϵ_1 and magnetic permeability μ_1, and a lossless MM with arbitrary values of electric permittivity ϵ_2 and magnetic permeability μ_2. These regimes correspond to different regions of the ϵ-μ diagram shown in Fig. 1, where $\epsilon=\epsilon_2/\epsilon_1$ and $\mu=\mu_2/\mu_1$. Regions B, C, D, and F correspond to transparent MMs with negative index of refraction. SPs occur for *s* polarization in regions B and F, and for *p* polarization in regions C and D.[16–19] Regions C and F support *backward* SPs, with a total-energy flux parallel to the MM interface, which is opposed to the direction of wave propagation.[16,17] As it happens in regions corresponding to conventional materials, regions B and D support *forward* SPs, for which the total-energy flux parallel to the MM interface is in the same direction as that of wave propagation. Region G (for *p* polar-

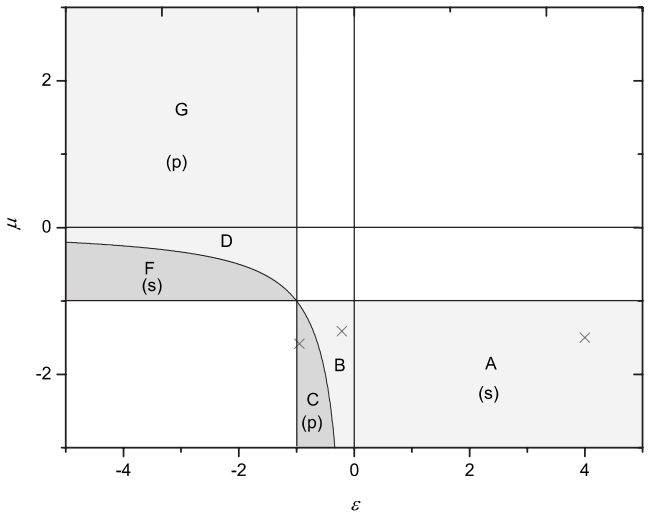

FIG. 1. SP regimes for a flat interface between a lossless conventional material (ϵ_1 and μ_1) and a lossless MM with arbitrary values of electric permittivity and magnetic permeability (ϵ_2 and μ_2). The axis are $\epsilon=\epsilon_2/\epsilon_1$ and $\mu=\mu_2/\mu_1$. The crosses indicate the regimes considered in the examples.

ization) includes the well-known case of electric conductors, whereas region A (for *s* polarization) corresponds to their magnetic analog. Note that there is no region where both *s*- and *p*-polarized SPs coexist simultaneously.

Because of their fundamental properties as well as their potential applications, the study of SPs is a topic of continually increasing interest. In areas such as condensed matter and surface physics, SPs have played a key role in the interpretation of a wide variety of experiments and in the understanding of various fundamental properties of solids. SPs have also found application in a wide spectrum of studies ranging from chemical sensors and biosensing to scanning tunneling microscopy and can serve as a basis for constructing nanoscale photonic circuits that will be able to carry optical signals and electric currents.[5] SPs might also be used, as is the case for conventional materials, to probe MMs characteristics and are expected to play an important role in many applications involving MMs, such as superlenses[20] or transparency and invisibility coatings.[21] In particular, the enhancement of evanescent waves by SPs is considered a key precursor for superlensing.[22]

As a consequence of the evanescent decay on both sides of the interface, the wave vector needed to excite the SP is always greater than that available to incident electromagnetic radiation. To overcome this fact, special phase matching techniques, such as prism or grating coupling, have been extensively used in the metallic case.[1–4] The unusual properties of MMs require that these techniques be reexamined in order to include all types of SPs that might be excited at the interface of isotropic MMs. Prism coupling (attenuated total reflection configuration) involving MMs has been considered in Refs. 19 and 23–25. Our aim is to reexamine the grating coupling mechanism in order to include the new SP regimes identified in Fig. 1.

Several methods, originally developed for conventional materials, have been applied for modeling the diffraction from corrugated gratings made of isotropic MMs exhibiting negative refraction.[26–29] One example of excitation of SPs in corrugated gratings has been provided in Ref. 28 to illustrate the dramatic changes that may occur in the diffraction efficiencies when the grating material is transformed from positive to negative index type. However, a comprehensive examination of the grating coupling mechanism including all the SP existence regions identified in Fig. 1 has not been presented in the literature yet.

To reexamine the grating coupling mechanism in the new SP regimes originating from the emergence of MMs, we first summarize the properties of SPs along the flat interface between a conventional material and a MM in Sec. II, providing a brief description of the boundary-value problem for the diffraction of a plane wave when the interface is periodically corrugated. In the following sections, we present numerical results obtained under conditions of resonant coupling: Sec. III is devoted to analyze *s*-polarized forward SPs occurring in Regime A, Sec. IV is devoted to analyze *s*-polarized forward SPs occurring in Regime B and Sec. V is devoted to analyze *p*-polarized backward SPs occurring in Regime C. For each regime, we show curves of efficiency and phase of the diffracted field as functions of the angle of incidence, obtained using the differential method[30] and incorporating the changes made in Ref. 28 in order to include media with negative indices of refraction. Both known and new behaviors are observed and discussed in the frame of the zero pole phenomenological model.[31–33] For conventional materials, the excitation of SPs in prism and grating coupling configurations is detected as a minimum in the reflected light. Our results show that this is not always the case for MMs. We have found situations where the resonant excitation of SPs exhibits optical responses that are very different from those obtained for the conventional metallic case. Particular attention is paid to the existence of a critical corrugation height leading to almost total absorption of the incident plane wave.[32–35] For conventional materials, the value of this critical corrugation height is almost the same as that corresponding to maximal intensity of the SP. Confirming conventional intuition, we find the existence of critical values of corrugation height for total absorption in all the SP regimes explored. For the regimes considered in Sec. III (regime A) and Sec. IV A (regime B) we find that the effects of SP excitation are very similar to those observed for natural materials. However, our numerical examples show that MMs with a negative index of refraction introduce some counterintuitive features, such as strong angular asymmetries in the absorption curves. Moreover, we have found SP regimes where maximal absorption of the incident wave and maximal intensity of the excited SP may occur at quite different values of corrugation height, with maximal intensity associated with maximum reflectivity, instead of almost total absorption. By fitting the phenomenological model to our numerical results, in Sec. VI we obtain information about the complex zeroes and poles of scattering matrix in the considered SP regimes. Concluding remarks are provided in Sec. VII. An $\exp(-i\omega t)$ time-dependence is implicit throughout the paper, with ω as the angular frequency, t as the time, and $i=\sqrt{-1}$. The symbols Re and Im are used for denoting the real and imaginary parts of a complex quantity, respectively.

II. GRATING COUPLED SPs

In the rectangular coordinate system (x,y,z), we consider the periodically corrugated boundary $y=f(x)=f(x+d)$ between a conventional material $[y>f(x)$, electrical permittivity ε_1, and magnetic permeability $\mu_1]$ and a MM $[y<f(x)$, electrical permittivity ε_2, and magnetic permeability $\mu_2]$, with d being the corrugation period. Both materials are homogeneous, isotropic, and linear. In this first study we confined ourselves to the widely used sinusoidal shape $y=\frac{h}{2}\sin(\frac{2\pi}{d}x)$.

When the corrugation is absent $(h=0)$, this boundary can support SPs with electromagnetic fields in the form,

$$\phi(x,y)=\exp[i(\alpha x+\beta^{(1)}y)], \quad y>0, \tag{1}$$

$$\phi(x,y)=\exp[i(\alpha x-\beta^{(2)}y)], \quad y<0, \tag{2}$$

where $\phi(x,y)$ represents the z-directed component of the total electric field for the s-polarization case or the z-directed component of the total magnetic field for the p-polarization case, α is the propagation constant, and $\beta^{(1)}$ and $\beta^{(2)}$ are the transverse wave numbers given by

$$\beta^{(1)}=\left(\frac{\omega^2}{c^2}\epsilon_1\mu_1-\alpha^2\right)^{1/2}, \tag{3}$$

$$\beta^{(2)}=\left(\frac{\omega^2}{c^2}\epsilon_2\mu_2-\alpha^2\right)^{1/2}. \tag{4}$$

Evanescent decay on both sides of the interface generally requires

$$\mathrm{Im}[\beta^{(i)}]>0, \quad i=1,2. \tag{5}$$

In the ideal case of lossless media, $\beta^{(i)}$ are purely imaginary and

$$\alpha^2>\max\left\{\epsilon_1\mu_1\frac{\omega^2}{c^2},\epsilon_2\mu_2\frac{\omega^2}{c^2}\right\}. \tag{6}$$

Boundary conditions at the interface give the dispersion relations for SPs,[6]

$$\beta^{(1)}+\frac{1}{\sigma}\beta^{(2)}=0, \tag{7}$$

where $\sigma=\epsilon_2/\epsilon_1$ or $\sigma=\mu_2/\mu_1$ for the p- or the s-polarized SPs, respectively. For lossless media and in order to satisfy condition (5) and the dispersion relation (7) simultaneously, $\sigma<0$. In terms of the relative constitutive parameters $\epsilon=\epsilon_2/\epsilon_1$ and $\mu=\mu_2/\mu_1$, the dispersion relations for SPs can be rewritten in a more convenient form as

$$\alpha^2=\frac{\omega^2}{c^2}\epsilon_1\mu_1\begin{cases}\dfrac{\mu(\mu-\epsilon)}{\mu^2-1} & s\text{-polarization}\\ \dfrac{\epsilon(\epsilon-\mu)}{\epsilon^2-1} & p\text{-polarization}\end{cases}. \tag{8}$$

Note that, due to the bivalued character of $\beta^{(i)}$ $(i=1,2)$, Eqs. (7) and (8) are not equivalent: if Eq. (7) has a solution, then this solution is given by Eq. (8), but we can find solutions of Eq. (8), which do not satisfy Eq. (7). When losses are neglected, the regions of existence of SPs in the ϵ-μ space are obtained from conditions (5) and (6).[16,17] These regions are indicated in Fig. 1. Regions of existence of SPs for dissipative materials with small imaginary part of their constitutive parameters have been discussed in Ref. 19.

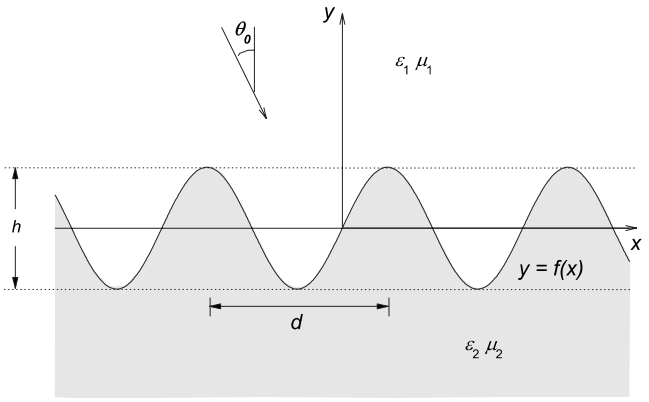

FIG. 2. Schematic illustration of the grating coupler.

Let us consider a linearly polarized electromagnetic plane-wave incident on the interface from region $y>0$ at an angle $\theta_0<\pi/2$ with respect to y axis. As indicated by condition (6), the SP propagation constant α is always greater than the projection along the interface of the incident wave vector, a fact that prohibits direct excitation of SPs by incident radiation on a flat interface. A periodic corrugation, such as that depicted in Fig. 2, provides the necessary wave-vector enhancement in multiples of $2\pi/d$.[1–4] Outside the corrugation region, the field $\phi(x,y)$ in the incident and in the transmission medium is represented by

$$\phi(x,y)=e^{i(\alpha_0x-\beta_0y)}+\sum_{m=-\infty}^{+\infty}R_me^{i(\alpha_mx+\beta_m^{(1)}y)}, \quad y>\max f(x), \tag{9}$$

and

$$\phi(x,y)=\sum_{m=-\infty}^{+\infty}T_me^{i(\alpha_mx-\beta_m^{(2)}y)}, \quad y<\min f(x), \tag{10}$$

where $\alpha_0=\frac{\omega}{c}\sin\theta_0$, $\alpha_m=\alpha_0+\frac{2\pi}{d}m$, $\beta_m^{(1)}=\sqrt{\frac{\omega^2}{c^2}\epsilon_1\mu_1-\alpha_m^2}$, $\beta_m^{(2)}=\sqrt{\frac{\omega^2}{c^2}\epsilon_2\mu_2-\alpha_m^2}$, and R_m and T_m are the complex amplitudes of the reflected and transmitted diffracted orders, to be determined by the solution of a boundary-value problem. In accordance with the Rayleigh hypothesis,[36] expansions (9) and (10) can be used in the boundary conditions, a procedure that leads to a system of linear equations for the complex amplitudes R_m and T_m.[26,27] However, as the validity of the Rayleigh hypothesis for negatively refracting gratings has not been established yet, to explore the coupling mechanisms between incident light and new surface polaritons on the dielectric-metamaterial interface we preferred to use the rigorous C-method[30,37] as reformulated in Ref. 28 to include media with negative indices of refraction. This method, not invoking the Rayleigh hypothesis, relies on the use of a new coordinate system that not only maps corrugated grating sur-

faces to planar surfaces, making the matching of boundary conditions easy, but also transforms Maxwell's equations in Fourier space into a matrix eigenvalue problem.[37] Incidentally, it should be noted that our implementation of the Rayleigh method gives results in good agreement with those obtained with the C-method for all cases presented here.

Only a finite number of diffracted orders in expansions (9) and (10) corresponds to propagating plane waves while the others have an evanescent nature. A coupling between incident radiation and a SP propagating along the grating with complex propagation constant $\alpha(h)$ is obtained when one of the evanescent orders is phase matched [Re $\alpha(h)=\alpha_m$] with the SP,

$$\text{Re } \alpha(h) = \frac{\omega}{c}\epsilon_1\mu_1 \sin\theta_0 + m\frac{2\pi}{d}, \tag{11}$$

where m is an integer. Assuming that the grating does not perturb the SP (which is the case for very shallow corrugations), $\alpha(h)$ in Eq. (11) can be replaced by $\alpha(0)$, the propagation constant of a SP along a flat interface given by Eq. (8). In terms of the dimensionless propagation constant $\kappa(h)=c\alpha(h)/\omega$, the coupling condition can be rewritten as

$$\sin\theta_0 + m\frac{\lambda}{d} = \text{Re } \kappa(h), \tag{12}$$

where λ is the wavelength in the medium of incidence.

To investigate the grating coupling mechanism in the new SP regimes provided by the emergence of MMs with arbitrary values of constitutive parameters, we consider the setup illustrated in Fig. 2. For the sake of simplicity, we chose the wavelength to period ratio λ/d in such a way that only the specularly reflected order [the plane wave with $m=0$ in Eq. (9)] propagates. It is well known that MMs are both dispersive and absorptive. Since we are interested in the impact of SPs on the reflectance as a function of the angle on incidence θ_0 at a single frequency, dispersion is irrelevant here. On the other hand, material absorption, set to zero to obtain the regime maps describing the SP dispersion relation (Fig. 1), must be set to a finite value to account for the inevitable loss of the MM in the region $y<f(x)$. To illustrate the coupling in different regimes, we consider interfaces with constitutive parameters ϵ and μ corresponding to regions A, B, and C in Fig. 1. These cases are indicated with crosses in Fig. 1. Examples for regimes D, F, and G, obtained, respectively, from regimes B, C, and A interchanging the relative material parameters $\epsilon \leftrightarrow \mu$ and the polarization $p \leftrightarrow s$ will be omitted. Taking into account that the equations governing regime A can be obtained from those governing regime G through an interchange between the values of the relative material parameters and the polarization, SP effects in regime A are expected to be magnetic analogs for s-polarized waves of the well-known SP effects occurring for metallic gratings illuminated by p-polarized radiation. Although our calculations confirm this expectation, we begin by discussing this case to establish first some known theoretical points and to address later the issue of similarities and differences between regimes associated with highly reflecting (constitutive parameters in regions A and G) and transparent (constitutive parameters in regions B, C, D, and F) surfaces.

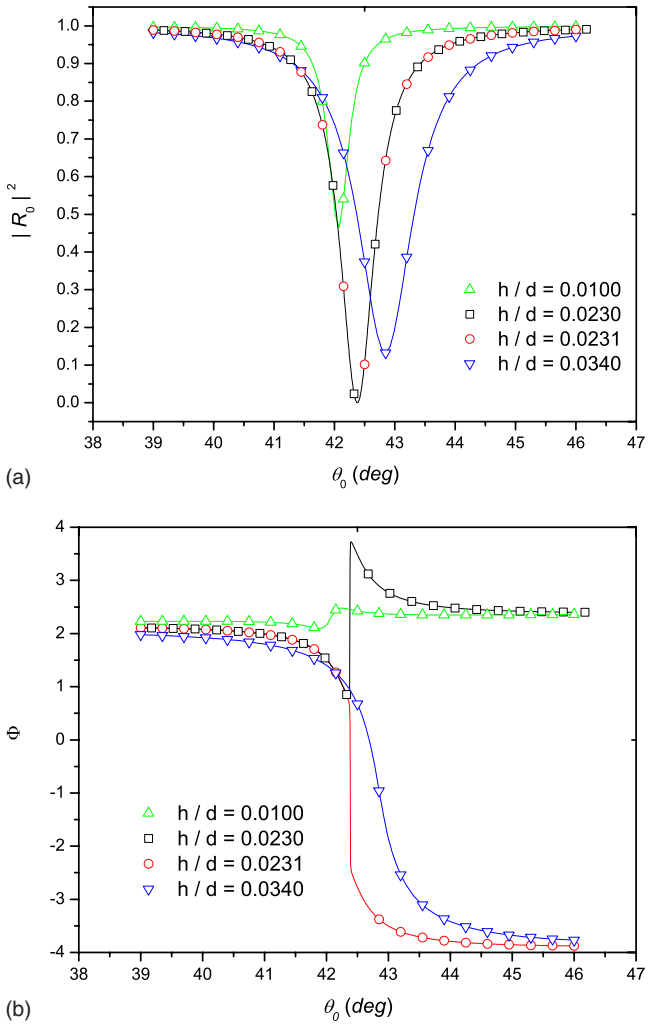

FIG. 3. (Color online) (a) Diffraction efficiency $|R_0|^2$ and (b) phase shift Φ in the specularly reflected order as functions of the angle of incidence θ_0 for s polarization, $\lambda/d=1.9$ and for different values of the groove depth to period ratio h/d. The relative constitutive parameters are $\epsilon=4+0.001i$ and $\mu_2=-1.5+0.001i$.

III. REGIME A: *s*-POLARIZED FORWARD SPs

First we choose $\lambda/d=1.9$ and constitutive parameters $\epsilon=4+0.001i$ and $\mu=-1.5+0.001i$, corresponding to regime A in Fig. 1 where SPs occur in s polarization. With these parameters, Eq. (8) gives a dimensionless propagation constant $\kappa(0)=\pm(2.56904+0.00223i)$ for the flat surface. Assuming $\kappa(0)\approx\kappa(h)$, Eq. (12) predicts resonant coupling with SPs at an angle of incidence $\theta_0\approx 41.99°$. Our calculations confirm this expectation, as can be seen in Fig. 3 where we show plots of the efficiency $|R_0|^2$ and the phase shift Φ in the specularly reflected order as functions of the angle of incidence θ_0 for s polarization and for different values of the groove depth to period ratio h/d. The variation in the angular position of the dips for different corrugation heights indicates a variation in the real part of the SP propagation constant,

whereas the variation in the half width of the dips indicates a variation in the imaginary part of the SP propagation constant. Almost identical efficiency curves with very pronounced dips (computed minima $\approx 10^{-8}$) can be observed for $h/d=0.0230$ and 0.0231 at an angle of incidence very close to that predicted by Eq. (12) with the quasiplane approximation $\kappa(0)\approx\kappa(h)$. Both dips are accompanied by phase shifts $\Phi\approx\pi$, but the phase curve for $h/d=0.0230$ exhibits a maximum and a minimum, whereas for $h/d=0.0231$ the phase is a decreasing function of the angle of incidence. For other values of h/d the dips are not so pronounced although they still occur for similar angles of incidence. The phase curve for $h/d=0.01$ exhibits a maximum and a minimum, but there is no maximum or minimum for $h/d=0.034$. Apart from a change in the polarization of the incident wave, the features shown in Fig. 3 are the magnetic analog of the phenomenon of total absorption of a monochromatic wave by a metallic grating,[32–35] in which a very weak corrugation of a highly reflecting flat surface causes the reflectance to fall dramatically to zero.

It is well established nowadays that the phenomenon of total absorption by a metallic grating can be understood with a phenomenological theory (see Refs. 32 and 33, and references therein) based on the computation in the complex plane of the poles and zeros of the scattering matrix. For the case of a metallic grating supporting only the specularly reflected order and illuminated under p-polarization, the complex amplitude R_0 can be represented by the following phenomenological expression:

$$R_0(z,h/d)=\xi(z,h/d)\frac{z-z_0(h/d)}{z-z_p(h/d)}, \tag{13}$$

where z is the complex extension to the complex plane of $\sin\theta_0$, z_0, and z_p denote the complex zero and pole of R_0, respectively, and $\xi(z,h/d)$ is a complex regular function near z_0 and z_p, which does not change noticeably near $z=z_p$. The pole $z_p(h/d)$ and the dimensionless propagation constant $\kappa(h)=c\alpha(h)/\omega$ differ only in multiples of the wavelength to period ratio λ/d.

The complex numbers z_0 and z_p cannot be theoretically calculated from the grating parameters and must be numerically determined for each grating problem. Their determination could be carried out by means of any of the formalisms developed to predict the efficiency of a grating but requires the extension of these formalisms to the complex plane. For metallic gratings, the relation $\mathrm{Re}\ z_0\approx\mathrm{Re}\ z_p$ holds. The phenomenological expression (13) predicts total absorption whenever the imaginary part of $z_0(h/d)$ changes its sign as h/d is varied. If, for a given grating, $z_0(h/d)$, lies in the real axis, a plane wave illuminating the grating with $z=z_0$ will be totally absorbed, whereas if $\mathrm{Im}\ z_0\neq 0$, the incident wave will be partially absorbed. The curve of $\Phi(z)$ as a function of the angle of incidence shows a different behavior depending on whether $\mathrm{Im}\ z_0\ \mathrm{Im}\ z_p>0$ or $\mathrm{Im}\ z_0\ \mathrm{Im}\ z_p<0$. In the first case the phase curve presents a maximum and a minimum, while in the second case there are neither maxima nor minima. Therefore, by studying the phase curves, it is possible to visualize the trajectory of $z_0(h/d)$ in the complex plane when h/d is varied, something which could not otherwise be obtained from the efficiency curves alone.[35]

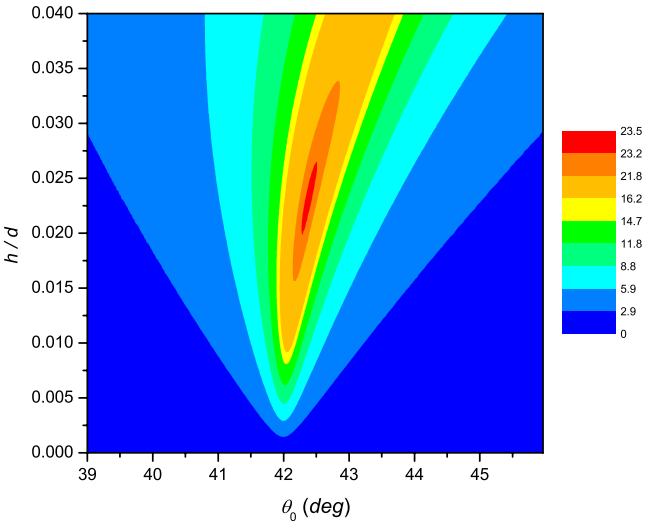

FIG. 4. (Color online) Map of $|R_{+1}|$ as a function of h/d and θ_0, the other parameters are as in Fig. 3.

Once the numerical values of $z_0(h/d)$ and $z_p(h/d)$ are known, Eq. (13) provides a simple expression for approximating the complex amplitude $R_0(z,h/d)$ to a good degree of accuracy. Conversely, it can also be used to estimate the numerical values of $z_0(h/d)$ and $z_p(h/d)$ by fitting the curves of $|R_0|^2$ and Φ near a SP resonance, thus providing some useful information about the behavior of SPs propagating along the corrugated surface.

Going back to our example, from the previous considerations we should conclude that, for gratings with material parameters in region A, the phenomenological expression (13) now describes the behavior of the complex amplitude R_0 in s polarization rather than in p-polarization, as was the case for gratings made of conventional metals. The existence of the pronounced dips at $\theta_0\approx 42.37°$ indicates that the complex zero crosses the real axis for some critical value of h/d between 0.0230 and 0.0231, where total absorption should be observed. From the phase curves shown in Fig. 3(b), we conclude that $\mathrm{Im}\ z_0\ \mathrm{Im}\ z_p>0$ for $h/d=0.0230$ (the curve presents a maximum and a minimum) and that for $h/d=0.0231$, $\mathrm{Im}\ z_0\ \mathrm{Im}\ z_p<0$ (monotonous curve).

It can be deduced from Eq. (12) that the evanescent order, which is phase matched with the SP [$\mathrm{Re}\ \alpha(h)=\alpha_m$], is represented by terms with $m=+1$ in expansions (9) and (10). Figure 4 shows a map of $|R_{+1}|$ as a function of θ_0 and h/d. For the case of metallic gratings supporting only a propagating order, the optimal excitation of SP occurs at almost the same conditions as total absorption and maximum local-field enhancement. The map in Fig. 4 clearly indicates that this is also the case in this example.

IV. REGIME B: *s*-POLARIZED FORWARD SPs

For our next example we have chosen an interface with relative constitutive parameters $\epsilon=-0.21213+0.001i$ and $\mu=-1.4142+0.001i$, corresponding to regime B in Fig. 1

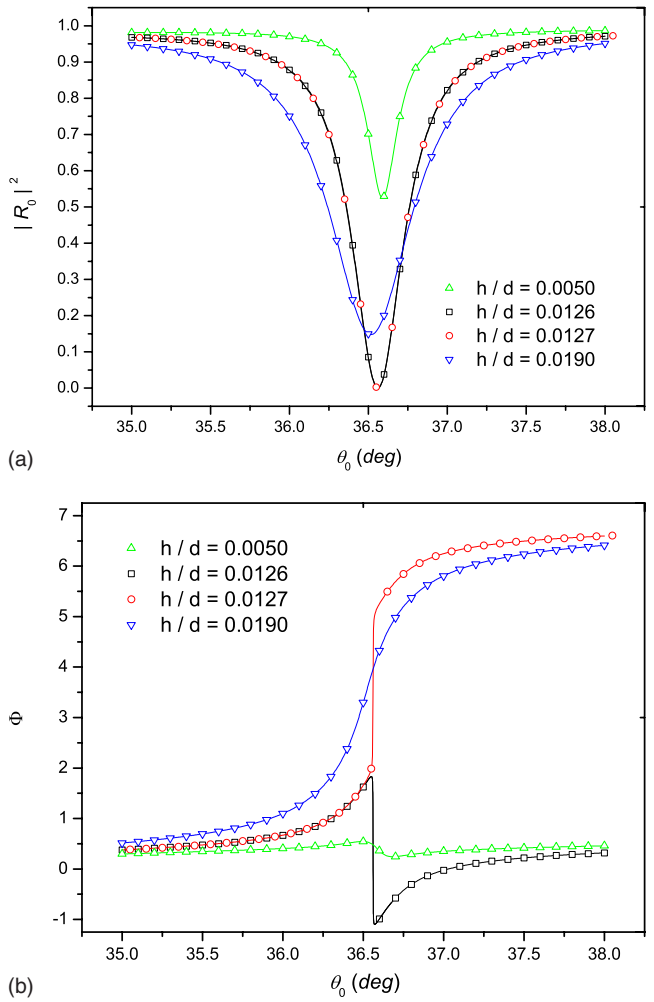

FIG. 5. (Color online) (a) Diffraction efficiency $|R_0|^2$ and (b) phase shift Φ in the specularly reflected order as functions of the angle of incidence θ_0 for s polarization, $\lambda/d=1.9$ and for different values of the groove depth to period ratio h/d. The relative constitutive parameters are $\epsilon=-0.21213+0.001i$ and $\mu=-1.4142+0.001i$.

where SPs occur in s polarization. Equation (8) gives $\kappa(0)=\pm(1.30385+0.00138i)$ for a flat surface with these parameters. Since the real part of the relative refractive index of this surface is less than one, the flat surface would exhibit very different reflectivities for angles of incidence less or greater than the critical angle of total reflection of 33.21°. By selecting the value of λ/d, we can tune the angle of incidence θ_0 for which a coupling between the incident wave and a SP is expected to fall in regions corresponding either to high ($\theta_0>33.21°$) or low ($\theta_0<33.21°$) reflectivity.

A. Excitation after total reflection

We first select the value $\lambda/d=1.9$, for which Eq. (12) with the quasiplane approximation predicts a resonant coupling near $\theta_0\approx 36.57°$, that is, in the region where the flat interface behaves as totally reflecting. The evanescent order, which is phase matched with the SP is represented by the terms with $m=-1$ in expansions (9) and (10). Figure 5 shows $|R_0(\theta_0)|^2$ and the phase shift $\Phi(\theta_0)$ corresponding to the specularly reflected order for s polarization and for different values of the groove depth to period ratio h/d in the range 0.0050–0.0190. Although the interface considered in this example is characterized by a basically real refractive relative index, the curves shown in Fig. 5 exhibit essentially the same features as those presented in Fig. 3 for an interface with a basically imaginary refractive index. Almost total absorptions (minima $\approx 10^{-8}$) occur for $h/d=0.0126$ and 0.0127 at an angle of incidence very close to the value predicted by the quasiplane approximation. Varying the value of h/d, the phase changes its behavior with the angle of incidence, from curves exhibiting a maximum and a minimum ($h/d=0.0100, 0.0126$) to monotonous curves ($h/d=0.0127$, 0.0190), a fact which indicates that the complex zero z_0 crosses the real axis at a critical value of h/d between 0.0126 and 0.0127, where total absorption should be observed. Figure 6 shows that, as it happens for metallic gratings and for the gratings considered in our previous example, the amplitude of the evanescent order, which is phase matched with the SP, takes its maximum value under conditions of total absorption, where we have verified that the maximum local-field enhancement also occurs.

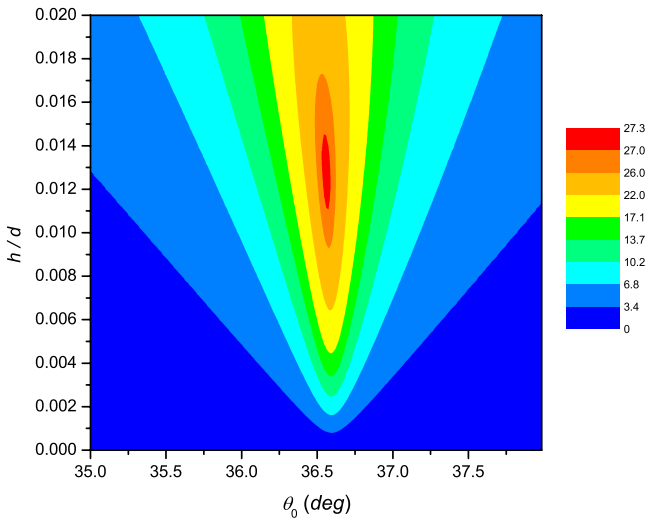

FIG. 6. (Color online) Map of $|R_{-1}|$ as a function of h/d and θ_0, the other parameters are as in Fig. 5.

B. Excitation before total reflection

To continue our study of the s-polarized forward SPs supported by a sinusoidally corrugated boundary with relative constitutive parameters in region B, we next consider a value $\lambda/d=1.5$, for which Eq. (12) with the quasiplane approximation predicts a resonant coupling near $\theta_0\approx 11.31°$. At this angle of incidence the flat interface reflects around 20% of the incident power instead of behaving as totally reflecting, as was the case in our previous example. The evanescent order, which is phase matched with the SP, is represented by the terms with $m=-1$ in expansions (9) and (10).

Figure 5 shows the efficiency $|R_0|^2(\theta_0)$ and the phase shift $\Phi(\theta_0)$ corresponding to the specularly reflected order and for different values of h/d in the range 0.0070–0.0280. The ef-

ficiency curve for a grating with $h/d=0.007$ still resembles the reflectivity curve of a flat surface, except at angles of incidence near the angle predicted by the quasiplane approximation for SP excitation, where a weak asymmetry, not present in efficiency curves obtained for conventional grating couplers nor for the MM grating couplers considered in our previous examples, is manifested by the presence of a minimum and a maximum. When h/d is increased from this value, we have observed [not shown in Fig. 5(a)] that the asymmetry in the efficiency curve becomes more and more pronounced, exhibiting a lower minimum and a higher maximum, until the minimum is zero within our computing precision. The efficiency curves for $h/d=0.0225$ and 0.0226 indicated in Fig. 5(a) are indistinguishable and exhibit a minimum $\approx 10^{-8}$, while the maximum reaches a value, which is more than twice the value of the reflectivity of the flat surface in this angular region. For greater values of h/d in the considered range, the minimum is nonzero while the value of the maximum increases, as can be seen in the curve shown for $h/d=0.0280$ for which the value of the maximum is almost three times the value obtained for $h/d=0$. This curious behavior has never been observed in gratings made of conventional materials, for which the absorption due to SP excitation is first reduced and eventually disappears when the groove depth to period ratio is increased from the critical value corresponding to total absorption. In terms of the pole zero phenomenological model, this rather unusual behavior of the efficiency curves near regions of SP excitation could be explained assuming that $\mathrm{Re}\, z_0 \neq \mathrm{Re}\, z_p$, contrary to what happens for metallic gratings for which $\mathrm{Re}\, z_0 \approx \mathrm{Re}\, z_p$.

As in our previous examples, the phase curves shown in Fig. 7(b) change their behavior at a critical value of h/d, in this case between 0.0225 and 0.0226. For values of h/d less than such a critical value, the curves show a maximum and a minimum, a behavior that should correspond to $\mathrm{Im}\, z_p\, \mathrm{Im}\, z_0 > 0$, while for values of h/d greater than this critical value the curves are monotonic functions of the angle of incidence. However, contrary to the behavior found in the previously described regimes, we observed that the amplitude of the evanescent order, which is phase matched with the SP, does not take its maximum value under the same conditions where maximal absorption of the incident wave occurs—a feature that should prevent us from obtaining maps of the SP dispersion relation by optically detecting the angular position of the minima, as is of common use in conventional prism and grating couplers.[1–5] This can be appreciated in Fig. 8, where we give maps of $|R_0|$ [Fig. 8(a)] and $|R_{-1}|$ [Fig. 8(b)] as functions of θ_0 and h/d. Note that the map in Fig. 8(a) reflects the asymmetries in the efficiency curves shown in Fig. 7(a).

V. REGIME C: *p*-POLARIZED BACKWARD SPs

Here we assume that the relative constitutive parameters are $\epsilon=-0.9487+0.0001i$ and $\mu=-1.5811+0.001i$, corresponding to regime C in Fig. 1 where backward SPs occur in p polarization. Using the Poynting vector associated with SPs, it can be shown that the total power flow along the interface is directed opposite to the direction of phase propagation in this regime.[16] For a flat surface with these parameters, Eq. (8) gives $\kappa(0)=\pm(2.44979-0.00245i)$. Choosing $\lambda/d=1.9$, Eq. (12) with the quasiplane approximation predicts a resonant coupling near $\theta_0 \approx 33.35°$. In this angular region, the flat interface reflects less than 3% of the incident power. The evanescent order, which is phase matched with the SP, is represented by the terms with $m=+1$ in expansions (9) and (10).

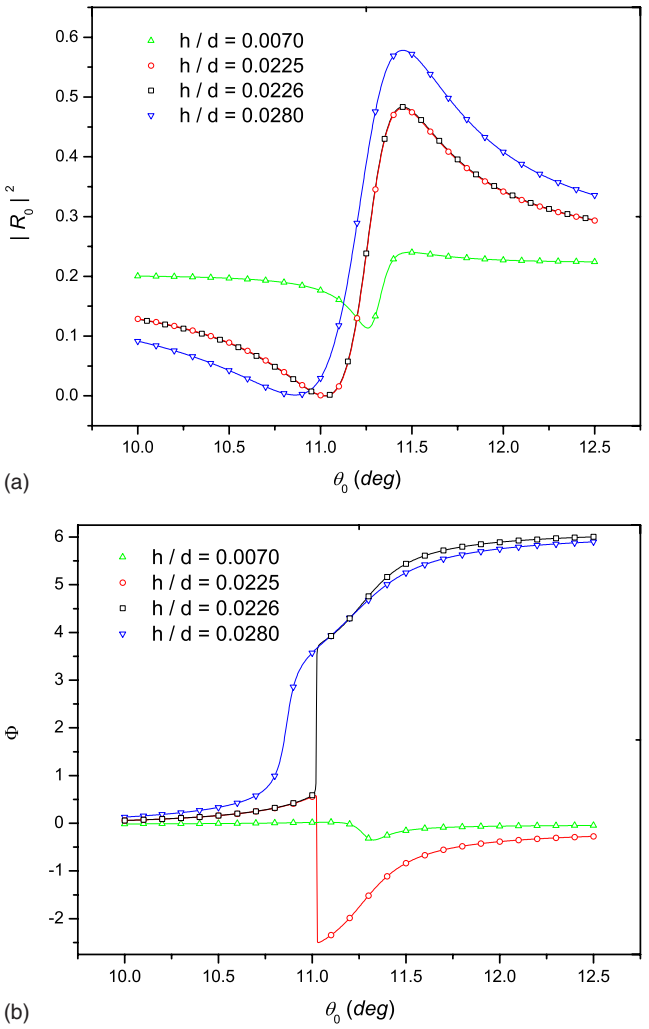

FIG. 7. (Color online) Same as Fig. 5 but for $\lambda/d=1.5$.

The specular reflectivity $|R_0(\theta_0)|^2$ of the sinusoidally corrugated interface is shown in Fig. 9(a) for p-polarized incident waves and for $h/d=0.001$, 0.00275, 0.00278, and 0.0036. All the curves exhibit minima near the angle of incidence, for which resonant coupling with SPs is expected. The angular position of these minima decreases as we increase h/d in this range. The curves for $h/d=0.00275$ and 0.00278 are indistinguishable and they present almost total absorptions (minima $\approx 10^{-8}$) at an angle of incidence $\theta_0=33.34°$. The corresponding curves of $\Phi(\theta_0)$ are shown in Fig. 9(b). Depending on the value of h/d, the phase changes its behavior with the angle of incidence, passing from curves exhibiting a maximum and a minimum ($h/d=0.001$, 0.00275) to monotonically increasing curves ($h/d=0.00278, 0.0036$). In terms of the phenomenological model,

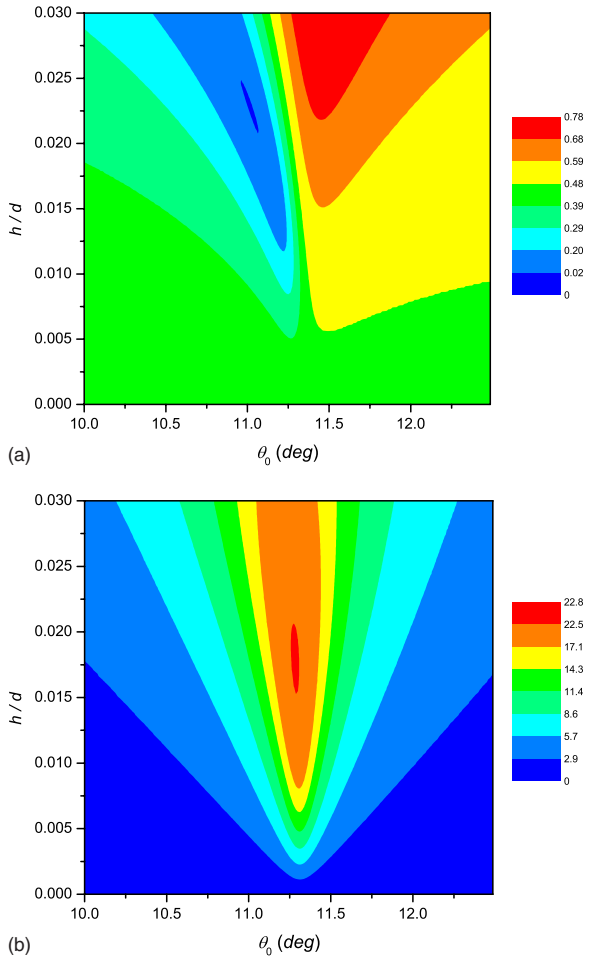

FIG. 8. (Color online) (a) Map of $|R_0|$ and (b) map of $|R_{-1}|$ as functions of h/d and θ_0, the other parameters are as in Fig. 7.

the behaviors shown in Figs. 9(a) and 9(b) seem to indicate the existence of a real zero z_0 at a critical value of h/d between 0.00275 and 0.00278, where total absorption should be observed.

SP-mediated total absorption effects observed in gratings made of conventional metals are quite dramatic in the sense that the introduction of a weak corrugation in an otherwise highly reflecting surface can turn its reflectivity into zero. The examples we have presented in Secs. III and IV A—where electromagnetic waves incident on the surface without corrugation suffer reactive attenuation and are reflected—exhibit the same characteristics. Compared with these examples, the SP-mediated total absorption effect shown in Fig. 9(a) seems to be far less interesting since the reflectivity of the surface is already very low without corrugation, and the excitation of the SP via a corrugation, although leading to total absorption, does not appear to change the optical response of the surface so dramatically. However, we have observed that the resonant excitation of the backward SP via a weak corrugation can also have a noticeable effect on the optical response of the surface. This is shown in Fig. 9(c), where we have plotted the specular reflectivity $|R_0(\theta_0)|^2$ for the same parameters as in Fig. 9(a), except now for groove depth to period ratios h/d=0.0054, 0.0061, and 0.0069. The corresponding phase curves (not shown) exhibit a monotonically increasing behavior, similar to that shown in Fig. 9(b) for h/d=0.00278 and 0.0036. We observe that the efficiency curves shown in Fig. 9(c) now exhibit maxima near the angle of incidence, for which resonant coupling with SPs is expected and where the efficiency curves shown in Fig. 9(a) exhibited minima. The angular position of these minima decreases as we increase h/d in this range. This curious behavior has never been observed in gratings made of conventional

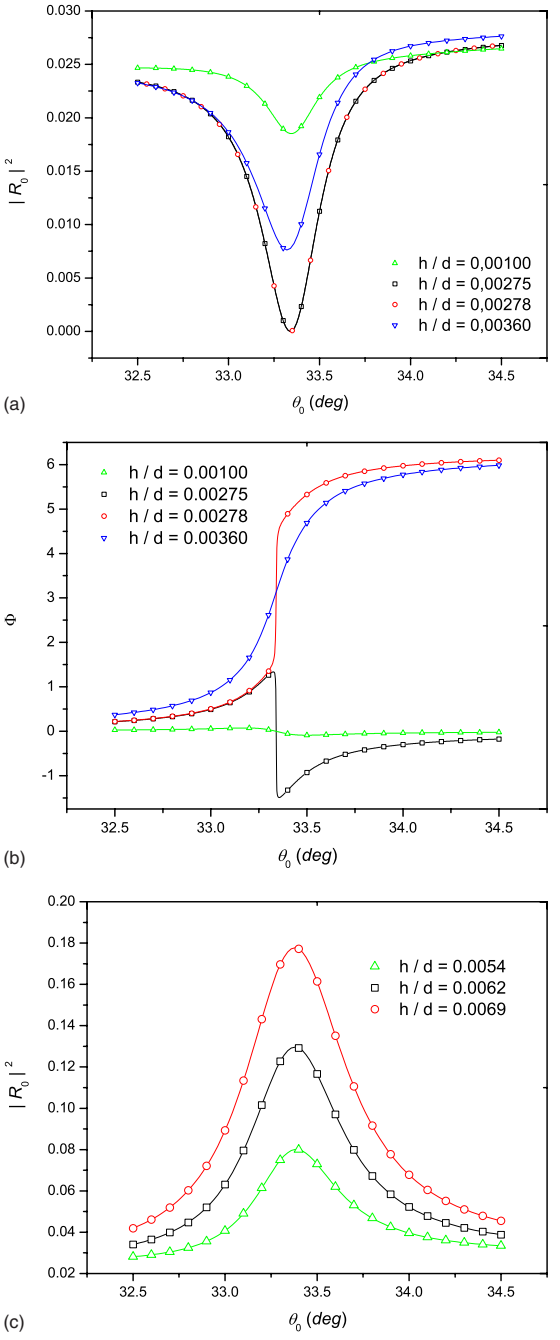

FIG. 9. (Color online) (a) Diffraction efficiency $|R_0|^2$ and (b) phase shift Φ in the specularly reflected order as functions of the angle of incidence θ_0 for p polarization, λ/d=1.9 and h/d =0.0010, 0.00275, 0.00278, and 0.00360; (c) same as (a) but for h/d=0.0054, 0.0062, and 0.0069. The relative constitutive parameters are ϵ=−0.9487+0.0001i and μ=−1.5811+0.0001i.

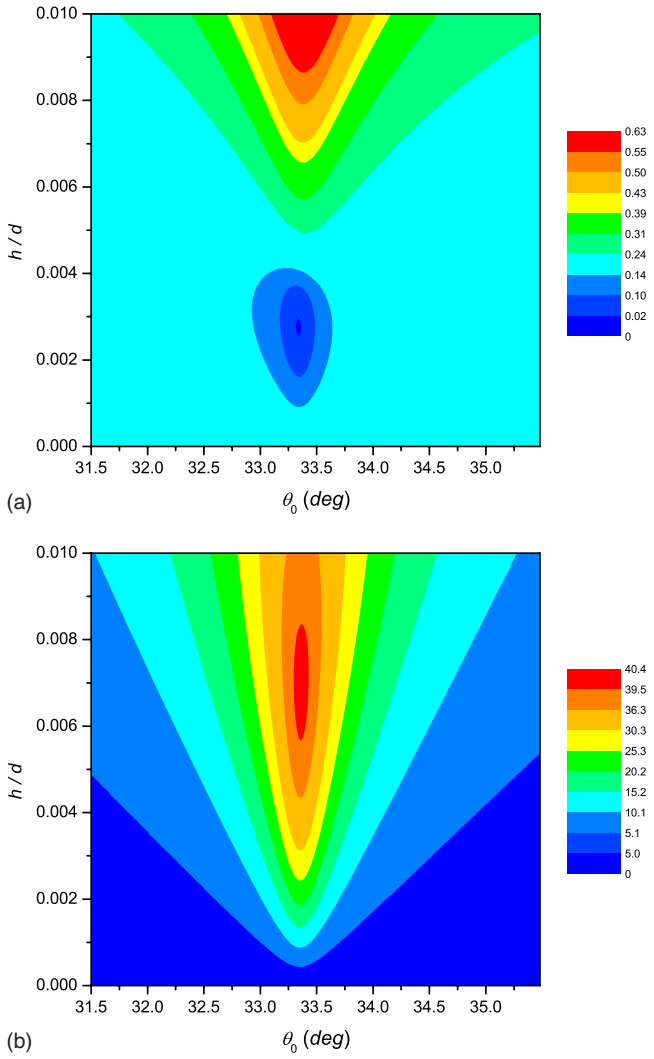

FIG. 10. (Color online) (a) Map of $|R_0|$ and (b) map of $|R_{+1}|$ as functions of h/d and θ_0, the other parameters are as in Fig. 9.

materials, for which the absorption due to SP excitation is first reduced and eventually disappears when the groove depth to period ratio is increased from the critical value corresponding to total absorption. Since all the efficiency curves shown in Fig. 9 are quite symmetrical, we should expect Re $z_0(h/d) \approx$ Re $z_p(h/d)$ for all the h/d values considered in this example. Moreover, for values of h/d giving a high reflectivity, we should expect the imaginary part of the zero to be appreciably greater than the imaginary part of the pole.

In Fig. 10 we show maps of $|R_0|^2$ [Fig. 10(a)] and $|R_{+1}|^2$ [Fig. 10(b)] as functions of θ_0 and h/d, which indicate that in this example, as was the case for the regime considered in Sec. IV B, maximal absorption of the incident wave and maximal intensity of the excited SP do not occur under the same conditions.

VI. FITTING THE PHENOMENOLOGICAL MODEL

The numerical determination of the model parameters $z_0(h/d)$ and $z_p(h/d)$ for the MM gratings considered in the previous sections requires us to perform an extension to the complex plane of the formalism used to predict the grating efficiency. In particular, $z_p(h/d)$ is intimately connected with the SP propagation constant $\kappa(h)=c\alpha(h)/\omega$, a quantity that can be obtained from the solution to the homogeneous problem[32,33] for the corrugated surface. Although it is not our intention to perform such a task here, we believe it is worth finding these parameters in an approximate manner by fitting the phenomenological expression (13) to our numerical results. To do so, we applied the phenomenological model and used a parameter fitting method to obtain the best values of $z_0(h/d)$, $z_p(h/d)$, and $\xi(z,h/d)$ that reproduce the numerical data predicted by our rigorous code. Some results for $z_0(h/d)$ and $z_p(h/d)$ in the different SP regimes previously considered are presented in Table I, the values for $\xi(z,h/d)$ (not shown) being almost identical to those provided by the Fresnel coefficients corresponding to a flat interface in the same angular region. We used an iterative scheme in which the model parameters extracted from the efficiency curve are introduced into Eq. (13) to calculate the model phase curve, the scheme being stopped when the model and the rigorously calculated phase curves agree within plot precision. We also present in Table I the complex quantity $z_p(0)$, obtained by shifting $\kappa(0)$ in multiples of the wavelength to period ratio λ/d until its real part falls in the interval (0,1). If the SP complex propagation constant were not affected by the sinusoidal corrugation, $z_p(0)$ should be equal to $z_p(h)$.[32,33] Due to the radiation losses introduced by the sinusoidal corrugation, the values of $|\text{Im } z_p(h/d)|$ presented in Table I are always greater than the values $|\text{Im } \kappa(0)|$ corresponding to the flat surface. The angular symmetries observed in the efficiency curves in the cases presented in Sec. III are reflected in Table I, in good agreement (up to the fourth significant figure) between the values Re $z_p(h/d)$ and Re $z_0(h/d)$. On the other hand, for the case presented in Sec. IV B the agreement between the values Re $z_p(h/d)$ and Re $z_0(h/d)$ is not so good

TABLE I. Results for $z_p(h/d)$ and $z_0(h/d)$ obtained by the fitting of the specular reflectivity data corresponding to some of the examples given in the different SP regimes presented in Secs. III, IV A, IV B, and V.

Section	λ/d	h/d	Re $z_p(h/d)$	Im $z_p(h/d)$	Re $z_0(h/d)$	Im $z_0(h/d)$	Re $z_p(0)$	Im $z_p(0)$
III	1.9	0.023	0.67377	0.00447	0.67376	7.610^{-6}	0.66904	0.00223
IV A	1.9	0.012	0.59547	−0.00263	0.59546	-1.310^{-4}	0.59615	−0.00138
IV B	1.5	0.022	0.19530	−0.00356	0.19129	-8.010^{-5}	0.19615	−0.00138
V	1.9	0.003	0.54967	−0.00300	0.54935	5.110^{-4}	0.54978	−0.00245
V	1.9	0.0069	0.54963	−0.00490	0.54814	0.01214	0.54978	−0.00245

(up to the second significant figure), a fact that accounts for the angular asymmetries observed in the efficiency curves for this example. In regime C (Sec. V) and for the value $h/d=0.0069$ greater than the one corresponding to total absorption, $|\mathrm{Im}\, z_0(h/d)|$ is appreciably greater than $|\mathrm{Im}\, z_p(h/d)|$. Taking into account that in this case $\mathrm{Re}\, z_0(h/d) \approx \mathrm{Re}\, z_p(h/d)$, the value of the maximum observed in the efficiency curve shown in Fig. 9(c) is $\approx |\xi\, \mathrm{Im}\, z_0/\mathrm{Im}\, z_p|^2$, which is appreciably greater than the reflectivity of the flat interface.

VII. CONCLUSION

In conclusion, we have studied the excitation of SPs at a sinusoidally corrugated interface separating a conventional dielectric and a MM with arbitrary values of permittivity and permeability, reexamining the grating coupling mechanism in order to include the new SP regimes provided by the emergence of MMs. Using a rigorous electromagnetic code, we have provided numerical examples evidencing the strong impact of SPs on the electromagnetic response of the interface, even for very shallow corrugations. Particular attention has been paid to conditions leading to total absorption of the incident power and to near-field enhancements. In those regimes, in which electromagnetic waves incident on the surface without corrugation suffer reactive attenuation and are therefore highly reflected, we have found SP effects with very similar characteristics to those previously found for corrugated metallic gratings where the introduction of a weak corrugation in an otherwise highly reflecting surface can turn its reflectivity to zero. However, new SP effects—not reported before to our knowledge—were identified in regimes corresponding to ideally transparent MMs with a negative index of refraction. We have found that in these regimes, contrary to the case of metallic gratings, the introduction of a weak corrugation in an otherwise poorly reflecting surface can produce high reflectivities in angular regions corresponding to coupling with SPs, demonstrating that SP effects could be used to effectively tune the optical properties of negative index materials. Furthermore, we have found that maximal absorption of the incident wave and maximal intensity of the excited SP do not occur under the same conditions. From a physical point of view, the SP resonant response of weakly corrugated surfaces such as those considered in this paper can be considered as the superposition of two main contributions: one originating in the fields reflected by the flat surface and the other in the fields radiated—via corrugation—by the SP. Thus, the differences between the resonant response for the highly reflecting and the transparent cases evidence the different kind of interference processes occurring between the fields radiated by the SP and the fields reflected by the surface without corrugation in both cases. To be able to consider all the new SP regimes obtained by the recent development of MMs, we have chosen to perform our study by fixing the frequency of the incident wave while varying other parameters such as the angle of incidence and the corrugation height. We believe that this approach is particularly appropriate and, in our opinion, even superior to other alternatives where the frequency is varied since in the latter case the frequency dependences of the MM effective permittivity and permeability could make it difficult to tune the SP resonances in the different regimes. As in any resonance phenomenon, complementary information on the effects reported here can be obtained by studying the associated homogeneous problem, i.e., by finding the characteristics of the electromagnetic eigenmodes supported by the corrugated interface. Although we are planning to report the results of such study in a future paper, here we have restricted ourselves to perform an approximate analysis, in which the complex propagation constants of the electromagnetic eigenmodes supported by the corrugated interface have been obtained by fitting the phenomenological expression (13) to our numerical results. We believe that our results will be useful for a deeper understanding of the properties of SPs and that the SP effects we have demonstrated opens up possibilities for practical applications involving MMs.

ACKNOWLEDGMENTS

We acknowledge the financial support from Consejo Nacional de Investigaciones Científicas y Técnicas (CONICET), Agencia Nacional de Promoción Científica y Tecnológica (Grant No. BID 1728/OC-AR PICT-11-1785), and Universidad de Buenos Aires (UBA).

*cuevas@df.uba.ar
†rdep@df.uba.ar

[1] *Surface Polaritons: Electromagnetic Waves at Surfaces and Interfaces*, edited by V. M. Agranovich and D. L. Mills (North-Holland, Amsterdam, 1982).
[2] *Electromagnetic Surface Modes*, edited by A. D. Boardman (Wiley, New York, 1982).
[3] H. Raether, *Surface Plasmons on Smooth and Rough Surfaces and on Gratings* (Springer-Verlag, Berlin, 1988).
[4] S. A. Maier, *Plasmonics: Fundamentals and Applications* (Springer, New York, 2007).
[5] J. M. Pitarke, V. M. Silkin, E. V. Chulkov, and P. M. Echenique, Rep. Prog. Phys. **70**, 1 (2007).
[6] R. Ruppin, Phys. Lett. A **277**, 61 (2000).
[7] Opt. Express **11**, 639 (2003), special issue on Negative Refraction and Metamaterials, edited by J. Pendry.
[8] IEEE Trans. Microwave Theory Tech. **52**, 1418 (2005), special issue on Metamaterial Structures, Phenomena and Applications, edited by T. Itoh and A. A. Oliner.
[9] J. Opt. Soc. Am. B **23**, 386 (2006), special issue on Metamaterials, edited by V. M. Shalaev and A. Boardman.
[10] *Metamaterials: Physics and Engineering Explorations*, edited by N. Engheta and R. W. Ziolkowski (Wiley, New York, 2006).
[11] R. A. Depine and A. Lakhtakia, Microwave Opt. Technol. Lett. **41**, 315 (2004).
[12] D. R. Smith, W. J. Padilla, D. C. Vier, S. C. Nemat-Nasser, and

S. Schultz, Phys. Rev. Lett. **84**, 4184 (2000).
[13] G. Dolling, M. Wegener, C. M. Soukoulis, and S. Linden, Opt. Lett. **32**, 53 (2007).
[14] I. Tsukerman, J. Opt. Soc. Am. B **25**, 927 (2008).
[15] C. García-Meca, R. Ortuño, R. Salvador, A. Martínez, and J. Martí, Opt. Express **15**, 9320 (2007).
[16] S. A. Darmanyan, M. Nevière, and A. A. Zakhidov, Opt. Commun. **225**, 233 (2003).
[17] I. V. Shadrivov, A. A. Sukhorukov, Y. S. Kivshar, A. A. Zharov, A. D. Boardman, and P. Egan, Phys. Rev. E **69**, 016617 (2004).
[18] A. Ishimaru, S. Jaruwatanadilok, and Y. Kuga, Electromagn. Waves **pier-51**, 139 (2005).
[19] A. Ishimaru, J. R. Thomas, and S. Jaruwatanadilok, IEEE Trans. Antennas Propag. **53**, 915 (2005).
[20] D. R. Smith, J. B. Pendry, and M. C. K. Wiltshire, Science **305**, 788 (2004).
[21] A. Alù and N. Engheta, Phys. Rev. E **72**, 016623 (2005).
[22] N. Fang, H. Lee, C. Sun, and X. Zhang, Science **308**, 534 (2005).
[23] R. Ruppin, J. Phys.: Condens. Matter **13**, 1811 (2001).
[24] K. Park, B. J. Lee, C. Fu, and Z. M. Zhang, J. Opt. Soc. Am. B **22**, 1016 (2005).
[25] H. Zhang, Q. Wang, N. Shen, R. Li, J. Chen, J. Ding, and H. Wang, J. Opt. Soc. Am. B **22**, 2686 (2005).
[26] R. A. Depine and A. Lakhtakia, Opt. Commun. **233**, 277 (2004).
[27] R. A. Depine and A. Lakhtakia, Phys. Rev. E **69**, 057602 (2004).
[28] R. A. Depine and A. Lakhtakia, Optik (Jena) **116**, 31 (2005).
[29] R. A. Depine, A. Lakhtakia, and D. R. Smith, Phys. Lett. A **337**, 155 (2005).
[30] J. Chandezon, M. T. Dupuis, G. Cornet, and D. Maystre, J. Opt. Soc. Am. **72**, 839 (1982).
[31] A. Hessel and A. A. Oliner, Appl. Opt. **4**, 1275 (1965).
[32] D. Maystre, in *Electromagnetic Surface Modes*, edited by A. D. Boardman (Wiley, New York, 1982), Chap. 17.
[33] M. Nevière, in *Electromagnetic Theory of Gratings*, edited by R. Petit (Springer-Verlag, New York, 1980).
[34] M. Hutley and D. Maystre, Opt. Commun. **19**, 431 (1976).
[35] R. A. Depine, V. L. Brudny, and J. M. Simon, Opt. Lett. **12**, 143 (1986).
[36] Lord Rayleigh, Proc. R. Soc. London **79**, 399 (1907).
[37] L. Li, J. Chandezon, G. Granet, and J. Plumey, Appl. Opt. **38**, 304 (1999).